J Pharmacokinet Pharmacodyn (2009) 36:239–260
DOI 10.1007/s10928-009-9120-1

Nonlinear pharmacokinetics of therapeutic proteins resulting from receptor mediated endocytosis

Ben-Fillippo Krippendorff · Katharina Kuester · Charlotte Kloft · Wilhelm Huisinga

Received: 7 November 2008 / Accepted: 26 May 2009 / Published online: 25 June 2009

Abstract Receptor mediated endocytosis (RME) plays a major role in the disposition of therapeutic protein drugs in the body. It is suspected to be a major source of nonlinear pharmacokinetic behavior observed in clinical pharmacokinetic data. So far, mostly empirical or semi-mechanistic approaches have been used to represent RME. A thorough understanding of the impact of the properties of the drug and of the receptor system on the resulting nonlinear disposition is still missing, as is how to best represent RME in pharmacokinetic models. In this article, we present a detailed mechanistic model of RME that explicitly takes into account receptor binding and trafficking inside the cell and that is used to derive reduced models of RME which retain a mechanistic interpretation. We find that RME can be described by an extended Michaelis–Menten model that accounts for both the distribution and the elimination aspect of RME. If the amount of drug in the receptor system is negligible

Electronic supplementary material The online version of this article (doi: 10.1007/s10928-009-9120-1) contains supplementary material, which is available to authorized users.

Implementations of the models in Berkeley Madonna and Matlab are available online as supplementary material.

B.-F. Krippendorff · W. Huisinga (✉)
Hamilton Institute, National University of Ireland Maynooth, Maynooth, Ireland
e-mail: wilhelm.huisinga@nuim.ie

B.-F. Krippendorff
International Max-Planck Research School for Computational Biology and Scientific Computing, Berlin, Germany

K. Kuester · C. Kloft
Department of Clinical Pharmacy, Institute of Pharmacy, Martin-Luther-Universitaet Halle-Wittenberg, Halle, Germany

K. Kuester · C. Kloft
Freie Universitaet Berlin, Berlin, Germany

a standard Michaelis–Menten model is capable of describing the elimination by RME. Notably, a receptor system can efficiently eliminate drug from the extracellular space even if the total number of receptors is small. We find that drug elimination by RME can result in substantial nonlinear pharmacokinetics. The extent of nonlinearity is higher for drug/receptor systems with higher receptor availability at the membrane, or faster internalization and degradation of extracellular drug. Our approach is exemplified for the epidermal growth factor receptor system.

Keywords Recepter mediated endocytosis · Nonlinear pharmacokinetics · Michaelis–Menten · Therapeutic proteins · Biopharmaceuticals · Epidermal growth factor receptor · Nonlinear dispostition · Receptor trafficking · Antibodies

Introduction

In recent years, therapeutic proteins have been a major focus of research and development activities in the pharmaceutical industry [1]. Currently, approximately 100 therapeutic proteins have been approved for human use, most of them being biotechnology-derived drug products and many more are under development. Important classes of therapeutic proteins are monoclonal antibodies, growth factors, and cytokines. Generally, therapeutic proteins provide highly attractive but sometimes exceptional behavior in the body [2]: their significant therapeutic potential results from their ability to bind—with high affinity—to specific targets such as receptors or cell surface proteins. For many protein drugs receptor mediated endocytosis (RME) is an important route of cellular uptake and disposition [3]. RME is the process of binding of an endogenous or exogenous ligand to a receptor and subsequent internalization of the resulting complex forming an endosome. Within the cell, the complex may be recycled to the cell surface or intracellularly be cleaved [4, 5]. Receptor-mediated uptake plays a major role in the elimination of protein drugs from the body [3] and is suspected to be a major source for the nonlinear pharmacokinetic (PK) behavior that is observed in clinical data for numerous protein drugs [6].

When aiming at analyzing preclinical/clinical pharmacokinetic data of protein drug trials, typically *empirical* 1-, 2- or 3-compartmental models including linear and/or nonlinear disposition processes have been developed. Michaelis–Menten terms have often been used to analyze experimental data in order to account for the observed nonlinearity [7–11]. These models have been selected based on, e.g., established statistical criteria (such as maximum likelihood), the precision of estimates of model parameters, and in few cases on model evaluation techniques [12–15]. However, being empirical in nature, these models do not provide a mechanistic understanding of how the different processes of receptor trafficking contribute to the overall pharmacokinetic profile, which is expected to guide, e.g., lead optimization or the design of more efficient dosing regimens. Equally important, there is no theoretical background as to when use the different existing empirical models for nonlinearity.

Less often, models have been developed that also include mechanistic terms to account for nonlinear phenomena, most prominently in terms of target-mediated drug disposition (TMDD) models [16–18]. TMDD explicitly accounts for binding to

a target and potential degradation of the resulting complex. Although originally developed to describe effects of extensive drug target binding in tissues, TMDD has more recently gained interest as a model for saturable elimination mechanisms for specific peptide and protein drugs, including RME [6, 18, 19]. TMDD is a general approach for situations where the interaction of a drug with its target is considered to be relevant and might affect the concentration-time profiles. However, it does not explicitly take into account the particular features of receptor *trafficking* inside cells, such as recycling and sorting, i.e., the process by which receptors and ligands are either targeted for intracellular degradation or recycled to the surface for successive rounds of trafficking [20].

There is a considerable amount of literature about detailed mechanistic descriptions of receptor trafficking systems in the systems biology literature (see, e.g., [5, 21] and references therein). Based on these receptor trafficking systems, our approach is to build a general detailed mechanistic model of RME that takes into account the most relevant kinetic processes of drug binding and receptor trafficking inside the cell. Detailed models derived from the underlying biochemical reaction network have the advantage of a mechanistic interpretation of the kinetic processes and estimated parameters. In [22], a cell-level model of the cytokine granulocyte colony-stimulating factor (G-CSF) and its receptor was incorporated into a pharmacokinetic/pharmacodynamic model to allow for analyzing the life span and potency of the ligand in vivo. However, often these advantages come along with the disadvantage of containing more parameters which, e.g., in population PK analysis of clinal trials may result in poorer performance in the model selection process, since models containing more parameters are usually penalized by the corresponding model selection criteria.

The objective of this article is to develop a framework for RME that is specifically tailored to the needs in PK analysis of clinical trials by bridging the points of view in pharmacokinetics and systems biology. The aims are (i) to develop a detailed model that takes into account the most relevant processes in relation to receptor trafficking; (ii) to derive reduced models of RME which retain a mechanistic interpretation and are defined in terms of a few parameters only, (iii) to offer guidance as to when use them, and (iv) to analyze the impact of the different processes on the extent of nonlinearity. While our approach applies to many receptor systems in general, we will use the epidermal growth factor receptor (EGFR) signalling pathway to illustrate the approach. The EGFR system has been intensively studied over the past 20 years and is one of the most important pathways for cell growth and proliferation as well as angiogenesis and metastasis [23]. The EGFR system comprises a tyrosine kinase receptor, which is activated by a variety of ligands such as the epidermal growth factor (EGF) or the transforming growth factor-α (TGF-α) [24–26]. Mathematical modelling of the EGFR system has proven to be useful for both, measurement of rate constants [27] as well as to elucidate the effects of receptor trafficking as an input to downstream signalling cascades [21, 28]. From a therapeutic point of view, the EGFR system has shown to be a promising target in cancer therapy [29, 30]. Several agents, including therapeutic proteins such as monoclonal antibodies (mAbs), have been developed to specifically target the EGFR with some already approved for drug treatment [31–33].

Theoretical

Throughout the article, the term 'ligand' refers to both a physiological ligand as well as an exogenous drug ligand.

Detailed model of RME (Model A)

We propose the following detailed model of RME of a ligand as schematically represented in Fig. 1: the ligand L_{ex} is present in the extracellular space. The ligand reversibly binds to free receptor R_m at the cell membrane with association rate constant k_{on} to form the ligand–receptor complex RL_m that dissociates with rate constant k_{off}. The complex is internalized with the rate constant $k_{interRL}$ forming an endosome. The internalized ligand–receptor complex RL_i is either recycled to the membrane with the rate constant k_{recyRL}, degraded with the rate constant k_{degRL} to RL_{deg}, or dissociates with the rate constant k_{break}. The dissociation results in the subsequent degradation of the ligand L_{deg} and the availability of the free receptor R_i inside the cell. Free intracellular receptor R_i is recycled to the membrane with the rate constant k_{recyR} and free membrane receptor R_m is internalized with the rate constant k_{interR}. Inside the cell, the receptor R_i is produced with the rate k_{synth} and degraded with the rate constant k_{degR}.

Based on the law of mass action, the rates of change for the various molecular species are given by the following system of ordinary differential equations (ODEs):

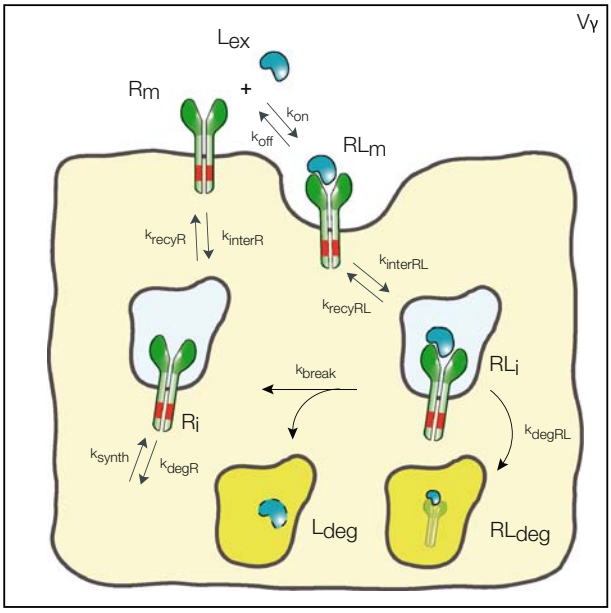

Fig. 1 Schematic representation of the detailed model of receptor mediated endocytosis. See text for description

$$dL_{ex}/dt = k_{off} \cdot RL_m - k_{on}/(V_\gamma N_A) \cdot R_m \cdot L_{ex} \quad (1)$$

$$dR_m/dt = k_{off} \cdot RL_m - k_{on}/(V_\gamma N_A) \cdot R_m \cdot L_{ex} + k_{recyR} \cdot R_i - k_{interR} \cdot R_m \quad (2)$$

$$dRL_m/dt = k_{on}/(V_\gamma N_A) \cdot R_m \cdot L_{ex} - k_{off} \cdot RL_m - k_{interRL} \cdot RL_m + k_{recyRL} \cdot RL_i \quad (3)$$

$$dRL_i/dt = k_{interRL} \cdot RL_m - k_{break} \cdot RL_i - k_{recyRL} \cdot RL_i - k_{degRL} \cdot RL_i \quad (4)$$

$$dR_i/dt = k_{interR} \cdot R_m - k_{recyR} \cdot R_i + k_{break} \cdot RL_i - k_{degR} \cdot R_i + k_{synth} \quad (5)$$

where N_A is Avogadro's number and V_γ is the volume of extracellular space per cell. In the above equations, all variables are expressed in number of molecules. All parameters are first-order rate constants in units [1/time] except for k_{synth}, which is a zero-order rate constant in units [molecules/time], and k_{on} which is a second-order rate constant in units [1/(concentration × time)]. The factor $1/(V_\gamma N_A)$ ensures conversion of units from molar concentration to number of molecules. With respect to the receptor, the above equations comprise the following three overall processes (cf. Fig. 1): (1) synthesis and degradation; (2) distribution of the different receptor species within and between the cytoplasm and the cell membrane; and (3) ligand–receptor interaction. With respect to the ligand, its disposition processes consist of the three overall processes: (i) binding to the receptor; (ii) internalization of the ligand–receptor complex; and (iii) intracellular degradation.

Reduced models of RME

One objective of this study is to derive and analyze reduced models of RME that capture the impact of receptor dynamics on the distribution and elimination of a ligand and that still allow for a *mechanistic* interpretation. While during short time intervals the transient redistribution processes between the different receptor species R_m, RL_m, RL_i and R_i may be of interest, these are usually assumed to be negligible on time scales of interest in pharmacokinetics. Therefore, our approach to reduce the detailed RME model will be based on the assumption that the receptor species R_m, RL_m, RL_i and R_i are in quasi-steady state. In order to finally derive reduced models of RME, it is necessary to make an additional assumption on the time-scale of receptor synthesis and degradation. We distinguish the following two scenarios: (1) the time scale of receptor synthesis and degradation is *slow* in comparison to the time scale of ligand disposition. In this case, we formally set $k_{synth} = k_{degR} = k_{degRL} = 0$. As a consequence, the total number of receptors in the system remains constant. Or, (2) the time scale of receptor synthesis and degradation is *fast*, i.e., comparable to the redistribution processes of the different receptor species. Both scenarios will be used in the following to establish a link between the reduced and the detailed model.

Reduced model of saturable distribution into the receptor system and linear degradation (Model B)

The idea in deriving a reduced model of RME is to use the quasi-steady state assumption for the receptor system (RS). This transforms the differential equations (2)–(5) into algebraic equations for R_m, RL_m, RL_i, R_i. For a given number of

extracellular ligand molecules L_{ex}, these algebraic equations can be solved explicitly. This allows us to compute the total number of ligand molecules in the receptor system $L_{RS} = RL_m + RL_i$ as a function of the extracellular number of ligands L_{ex}. Based on L_{RS}, the quasi-steady state number of intracellular ligand–receptor complexes RL_i can be computed, which determines the extent of elimination.

Model B (see Fig. 2) describes the evolution of the total number of ligands $L_{tot} = L_{ex} + L_{RS}$ in form of the following ODE:

$$dL_{tot}/dt = -k_{deg} L_{RS} \quad \text{with} \tag{6}$$

$$L_{RS} = \frac{B_{max} L_{ex}}{K_M + L_{ex}} \tag{7}$$

$$L_{ex} = \frac{1}{2}\left(L_{tot} - B_{max} - K_M + \sqrt{(L_{tot} - B_{max} - K_M)^2 + 4K_M L_{tot}}\right). \tag{8}$$

The equations comprise three parameters: the maximal ligand binding capacity B_{max} of the receptor system (in units molecules), the number of extracellular ligand molecules corresponding to a half-maximal binding capacity K_M (in units molecules), and the degradation rate k_{deg} (in units 1/time). In this reduced model the combination of saturable distribution and linear degradation results in the overall saturable elimination of the ligand.

For the two scenarios of *slow* or *fast* receptor synthesis and degradation, the functional relation between the parameters B_{max}, K_M and k_{deg} and the parameters of the detailed model of RME can be established. In the case of *slow* receptor synthesis and degradation, it is

$$B_{max} = R_0 \cdot \frac{k_{break} + k_{recyRL} + k_{interRL}}{k_{break} + k_{interRL} + k_{recyRL} + k_{interRL} \cdot k_{break}/k_{recyR}} \tag{9}$$

$$K_M = K_D \cdot \frac{V_\gamma N_A \cdot k_{break}\left(1 + \frac{k_{interRL}}{k_{off}} + \frac{k_{recyRL}}{k_{break}}\right)}{k_{break} + k_{interRL} + k_{recyRL} + k_{interRL} \cdot k_{break}/k_{recyR}} \tag{10}$$

$$k_{deg} = \frac{k_{break} \cdot k_{interRL}}{k_{interRL} + k_{break} + k_{recyRL}}, \tag{11}$$

where R_0 is the total number of receptors and $K_D = k_{off}/k_{on}$ denotes the dissociation constant of the ligand–receptor complex. In the case of *fast* receptor synthesis and degradation, the relation between the parameters is

$$B_{max} = \frac{k_{synth}}{k_{degR}} \cdot \frac{k_{recyR} \cdot (k_{recyRL} + k_{lyso} + k_{interRL})}{k_{interRL} \cdot (k_{lyso} + k_{recyR} \cdot k_{degRL}/k_{degR})} \tag{12}$$

$$K_M = K_D \cdot \frac{V_\gamma N_A \cdot k_{interR} \cdot (k_{recyRL} + k_{lyso} + k_{interRL} \cdot k_{lyso}/k_{off})}{k_{interRL} \cdot (k_{lyso} + k_{recyR} \cdot k_{degRL}/k_{degR})} \tag{13}$$

$$k_{deg} = \frac{k_{lyso} \cdot k_{interRL}}{k_{interRL} + k_{lyso} + k_{recyRL}}, \tag{14}$$

with $k_{lyso} = k_{break} + k_{degRL}$.

Reduced model of saturable degradation (Model C)

The proposed Model C (see Fig. 2) is a further reduction of Model B. It is based on the additional assumption that the amount of ligand distributed into the receptor system is negligible in comparison to the total amount of ligand molecules, i.e., $L_{\text{tot}} = L_{\text{ex}} + L_{\text{RS}} \approx L_{\text{ex}}$. More formally, Model C can be derived from Model B under the assumption

$$\frac{B_{\max}}{K_M + L_{\text{ex}}} \ll 1, \tag{15}$$

which implies $L_{\text{RS}} \ll 1$ and thus $L_{\text{tot}} \approx L_{\text{ex}}$ from Eq. 7. Substituting L_{ex} by L_{tot} in Eq. 7 and L_{RS} into Eq. 6 yields the ODE for the total number of ligand molecules:

$$\mathrm{d}L_{\text{tot}}/\mathrm{d}t = -\frac{V_{\max} L_{\text{tot}}}{K_M + L_{\text{tot}}}. \tag{16}$$

The model comprises two parameters: the maximal elimination rate of ligand molecules $V_{\max}$ (in units molecules/time) and the number of ligand molecules K_M, at which the elimination rate is half-maximal. Exploiting the relation

$$V_{\max} = k_{\text{deg}} \cdot B_{\max}, \tag{17}$$

we obtain the functional relations between $V_{\max}$ and the parameters of the detailed model of RME (Model A). In the case of *slow* receptor synthesis and degradation, the functional relationship is given by

$$V_{\max} = R_0 \cdot \frac{k_{\text{break}} \cdot k_{\text{interRL}}}{k_{\text{break}} + k_{\text{interRL}} + k_{\text{recyRL}} + k_{\text{interRL}} \cdot k_{\text{break}}/k_{\text{recyR}}} \tag{18}$$

and K_M is defined as in Eq. 10. In the case of *fast* receptor synthesis and degradation, it is

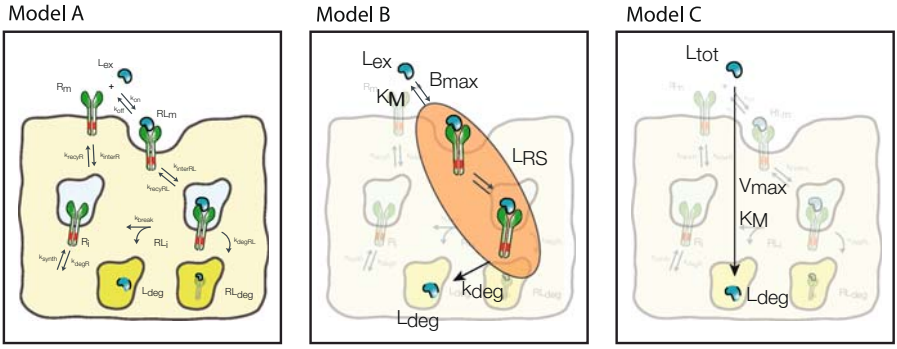

Fig. 2 Models of receptor mediated endocytosis of different resolution: Detailed model (Model A), reduced model of saturable distribution into the receptor system with linear degradation (Model B), and reduced model of saturable degradation (Model C). See text for details

$$V_{\max} = \frac{k_{\text{synth}}}{k_{\text{degR}}} \cdot \frac{k_{\text{lyso}} \cdot k_{\text{recyR}}}{k_{\text{lyso}} + k_{\text{recyR}} \cdot k_{\text{degRL}}/k_{\text{degR}}} \tag{19}$$

and K_M is defined as in Eq. 13.

Integration of RME into compartmental PK models

In order to facilitate the transfer of reduced models of RME into compartmental PK models underlying PK data analysis and for use in the example of therapeutic protein receptor interaction, we explicitly state the system of ODEs for a two-compartment PK model. The model comprises a central compartment (volume V_1 (in units volume) and ligand concentration C_1 (in units mass/volume)) from which linear elimination CL_{lin} (in units volume/time) takes place and a peripheral compartment (volume V_2 and total ligand concentration C_2), where saturable elimination via receptor mediated endocytosis CL_{RS} takes place (see Fig. 3). In the peripheral compartment, we further distinguish between the concentration C_{RS} within the receptor system and the extracellular concentration C_{ex}. The inter-compartmental transfer flows are denoted by q_{12} and q_{21} (in units volume/time).

As in this article we are interested in how to represent RME in PK models, the below mentioned system of ODEs based on the reduced Models B and C represent the proposed structural PK model that can be used for parameter estimation in PK data analysis of nonclinical and clinical trials. The parameter values are determined by performing a fit of the model to the specific in vivo data. Alternatively, the model might be used to scale-up in vitro derived RME parameter values to the in vivo situation (see also Discussion).

If Model B is used to describe the elimination by RME, the system of ODEs is

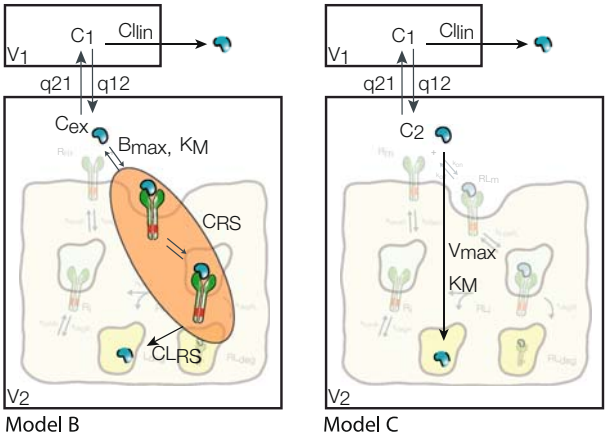

Fig. 3 Two two-compartment models with linear clearance from the central compartment and RME based on Model B (left) and Model C (right) in the peripheral compartment

$$V_1 \cdot \mathrm{d}C_1/\mathrm{d}t = q_{21} \cdot C_{\mathrm{ex}} - q_{12} \cdot C_1 - \mathrm{CL}_{\mathrm{lin}} \cdot C_1 + \mathrm{dosing} \tag{20}$$

$$V_2 \cdot \mathrm{d}C_2/\mathrm{d}t = q_{12} \cdot C_1 - q_{21} \cdot C_{\mathrm{ex}} - \mathrm{CL}_{\mathrm{RS}} \cdot C_{\mathrm{RS}}, \text{ with} \tag{21}$$

$$C_{\mathrm{RS}} = \frac{B_{\max} \cdot C_{\mathrm{ex}}}{K_M + C_{\mathrm{ex}}} \tag{22}$$

$$C_{\mathrm{ex}} = \frac{1}{2}\left(C_2 - B_{\max} - K_M + \sqrt{(C_2 - B_{\max} - K_M)^2 + 4K_M C_2}\right), \tag{23}$$

where dosing denotes a mass inflow (in units mass/time) of, e.g., an i.v. infusion over a given time. The parameter $B_{\max}$ denotes the total maximal ligand binding capacity in mass per volume or mol per volume, K_M denotes the concentration at which the binding capacity is half-maximal, $\mathrm{CL}_{\mathrm{lin}}$ and $\mathrm{CL}_{\mathrm{RS}}$ denote the total elimination capacities (in units volume/time) in the central and peripheral compartment, respectively. In terms of parameter estimation, the PK model contains eight parameters: V_1, V_2, q_{12}, q_{21}, $\mathrm{CL}_{\mathrm{lin}}$, $\mathrm{CL}_{\mathrm{RS}}$, $B_{\max}$ and K_M, plus additional variables relating to dosing.

If Model C is used to describe the elimination by RME, the system of ODEs is

$$V_1 \cdot \mathrm{d}C_1/\mathrm{d}t = q_{21} \cdot C_2 - q_{12} \cdot C_1 - \mathrm{CL}_{\mathrm{lin}} \cdot C_1 + \mathrm{dosing} \tag{24}$$

$$V_2 \cdot \mathrm{d}C_2/\mathrm{d}t = q_{12} \cdot C_1 - q_{21} \cdot C_2 - \frac{V_{\max} \cdot C_2}{K_M + C_2}, \tag{25}$$

where $V_{\max}$ denotes the total maximal elimination (in units mass/time), and all remaining parameters are defined as above. In terms of parameter estimation, the PK model contains seven parameters: V_1, V_2, q_{12}, q_{21}, $\mathrm{CL}_{\mathrm{lin}}$, $V_{\max}$ and K_M, in addition to the parameters relating to dosing.

Nonlinear PK caused by RME

In this section, we investigate the extent of nonlinearity in the context of the Michaelis–Menten model defined in Eqs. 24 and 25. We aim to examine the effect of drug and cell properties on the nonlinearity of the pharmacokinetics, e.g., different drug affinities to the receptor (different k_{on} and k_{off} values) or different rates of internalization and recycling of the drug in different cells.

In the chosen setting of the two-compartment PK model (cf. Eqs. 24 and 25, the total clearance $\mathrm{CL}_{\mathrm{tot}}$ is given by

$$\mathrm{CL}_{\mathrm{tot}} = \mathrm{CL}_{\mathrm{lin}} + \mathrm{CL}_{\mathrm{RS}} = \mathrm{CL}_{\mathrm{lin}} + \frac{V_{\max}}{K_M + C}, \tag{26}$$

where C denotes the relevant ligand concentration in the RME compartment (e.g., C_2 in Eq. 25). While the linear clearance is constant, the clearance attributed to RME varies between $V_{\max}/K_M$ for small ligand concentrations and 0 for high ligand concentrations. Therefore, we consider the quotient $V_{\max}/K_M$ as a measure of the extent of nonlinearity, i.e., the increase in total clearance for small ligand concentrations.

In order to jointly analyze the *slow* and the *fast* receptor synthesis and degradation scenario, we set

$$R_0 = R_m + R_i = \frac{k_{synth}}{k_{degR}} \cdot \left(1 + \frac{k_{interR}}{k_{recyR}}\right) \tag{27}$$

and replace the quotient k_{synth}/k_{degR} in Eq. 19 by $R_0/(1 + k_{interR}/k_{recyR})$ according to Eq. 27. Moreover, we extend the definition of k_{lyso} to the *slow* scenario by setting $k_{lyso} = k_{break}$ in this case (note: for the *fast* scenario $k_{lyso} = k_{break} + k_{degRL}$). Then, the extent of nonlinearity for both, the *fast* and the *slow* scenario, is given by

$$\frac{V_{max}}{K_M} = \frac{R_0}{V_\gamma N_A} \cdot \frac{k_{on}}{\frac{k_{off}}{k_{interRL}}\left(1 + \frac{k_{recyRL}}{k_{lyso}}\right) + 1} \cdot \left(\frac{1}{\left(1 + \frac{k_{interR}}{k_{recyR}}\right)\left(\frac{k_{interR}}{k_{recyR}}\right)}\right)^p, \tag{28}$$

where $p = 0$ for the *slow* scenario and $p = 1$ for the *fast* scenario. The above equation allows us to study in detail the influence of the various parameters on the extent of nonlinearity.

It can be inferred from Table 1 that ligand-specific, receptor system-specific as well as mixed parameters influence the extent of nonlinearity of the PK: nonlinearity increases for higher affinity drugs (k_{on}) and cell types, which have a higher receptor concentration at the surface of the cell membrane (R_0, k_{recyR}) and faster degradation processes (k_{lyso}). In contrast, higher values of k_{off}, k_{recyRL} and higher k_{interR}, k_{degR} will decrease the extent of nonlinearity by resulting in a lower number of intracellular ligand receptor complexes, free receptor molecules, or a smaller number of receptor molecules at the cell surface membrane.

In order to more clearly highlight the contribution of the dissociation constant K_D, we also give the following alternative representation of Eq. 28:

$$\frac{V_{max}}{K_M} = \frac{R_0}{V_\gamma N_A} \cdot \frac{1}{K_D} \cdot \frac{1}{\frac{1}{k_{interRL}}\left(1 + \frac{k_{recyRL}}{k_{lyso}}\right) + \frac{1}{k_{off}}} \cdot \left(\frac{1}{\left(1 + \frac{k_{interR}}{k_{recyR}}\right)\left(\frac{k_{interR}}{k_{recyR}}\right)}\right)^p. \tag{29}$$

As can be inferred from the above relation, the extent of nonlinearity can be very different for ligands with the same dissociation constant K_D, but different absolute values of k_{off}. The difference depends on the relative magnitude of the two terms in the first denominator in Eq. 29, i.e., $1/k_{off}$ to $1/k_{interRL} \cdot (1 + k_{recyRL}/k_{lyso})$.

Table 1 Contribution of the different parameters to the extent of nonlinearity

With increasing value of the corresponding parameter the extent of nonlinearity will increase (↑) or decrease (↓). For each parameter, it is indicated by (RS) or (L) whether it is related to the receptor system or the ligand, respectively

Increase of parameter	Resulting change in extent of nonlinearity
R_0	↑ (RS)
k_{recyR}	↑ (RS)
k_{on}	↑ (L)
k_{lyso}	↑ (RS & L)
$k_{interRL}$	↑ (RS & L)
k_{off}	↓ (L)
k_{interR}	↓ (RS)
k_{recyRL}	↓ (RS & L)

Methods

In order to simulate Models A, B and C, we numerically solved the corresponding system of ODE's with Matlabs built-in ode15s integrator (The Mathworks, Inc., Natick/MA, USA, version 7.4). Parameter values for the reduced Models B and C were derived from those of Model A using the established relations (12)–(14), and (19) and (13), respectively. Subsequently, numbers of molecules where converted into concentrations (nM).

The models were compared based on the simulated extracellular drug concentration. The specific details of the simulation studies are given in the respective Result section to allow for an easier comparison.

EGFR system with endogenous/physiological ligand

The application of our approach is illustrated using the EGFR system as an example. The properties of the EGF/EGFR system will be analyzed using experimentally measured parameters for the degradation of the epidermal growth factor, binding to the epidermal growth factor receptor and subsequent internalization [20, 34]. The rate constants of the corresponding reactions are listed in Table 2.

Hendriks et al. [20, 34] explored EGF as ligand to measure rate constants of the EGFR system. Since receptor is degraded as a consequence of ligand degradation, we choose the scenario of *fast* receptor synthesis and degradation for all investigations, i.e., Eqs. 12–14 and 19. However, not all rate constants of the herein proposed detailed model of RME were *explicitly* measured in [20, 34]. Since EGF is predominantly degraded from the EGF-receptor complex [5] rather than from the free form, we set $k_{\text{break}} = 0$ resulting in $k_{\text{lyso}} = k_{\text{degRL}} \neq 0$. Since the parameter k_{synth} was not available in literature, we used the steady state assumption for the receptor system prior to any ligand administration and the experimentally measured steady state number of membrane receptor $R_{\text{m}}^{(SS)}$ [28] to determine k_{synth} using the relation $k_{\text{synth}} = k_{\text{degR}} \cdot R_{\text{i}}^{(SS)}$ with $R_{\text{i}}^{(SS)} = R_{\text{m}}^{(SS)} \cdot k_{\text{interR}}/k_{\text{recyR}}$. The initial number of receptors are $R_{\text{m}}(0) = R_{\text{m}}^{(SS)}$, $R_{\text{i}}(0) = R_{\text{i}}^{(SS)}$, and $RL_{\text{m}}(0) = RL_{\text{i}}(0) = 0$; the initial concentration of extracellular ligand is $L_{\text{ex}}(0) = 40$ nM.

Table 2 Parameter values for the EGF/EGFR system

Parameter	Numerical value
k_{on}	5.82 1/(nM h)
k_{off}	14.4 1/h
$R_{\text{m}}^{(SS)}$	2×10^5 molecules
k_{recyR}	3.84 1/h
k_{interR}	4.2 1/h
k_{degR}	0.96 1/h
k_{recyRL}	1.2 1/h
k_{interRL}	15 1/h
k_{degRL}	1.2 1/h
V_γ	4×10^{-10} 1/cell

All parameter values have been extracted from Hendriks et al. [20, 34] and Shankaran et al. [28]. See also section "RME for the EGF/EGFR system"

EGFR system with exogenous/therapeutic protein ligand

The analysis of drug-EGFR interaction are performed using data from the monoclonal antibody zalutumumab (2F8), as published by Lammerts van Bueren et al. [11]. Zalutumumab is a human IgG1 EGFR antibody that potently inhibits tumor growth in xenograft models and has shown encouraging antitumor results in a phase I/II clinical trial [35, 36]. We transformed the originally published system of difference equations [11, Supplement] into the corresponding continuous system of ordinary differential equations[1] (ODEs):

$$\frac{\mathrm{d}}{\mathrm{d}t}A_{\mathrm{pl}} = k_{\mathrm{ip}}A_{\mathrm{int}} - k_{\mathrm{pi}}A_{\mathrm{pl}} - k_{\mathrm{el}}A_{\mathrm{pl}} \tag{30}$$

$$\frac{\mathrm{d}}{\mathrm{d}t}A_{\mathrm{int}} = k_{\mathrm{pi}}A_{\mathrm{pl}} - k_{\mathrm{ip}}A_{\mathrm{int}} - k_{\mathrm{b}}\left(\frac{\widehat{B}_{\max}(A_{\mathrm{int}}/V_{\mathrm{int}})^h}{(A_{\mathrm{int}}/V_{\mathrm{int}})^h + K_{\mathrm{M}}^h} - A_b\right) \tag{31}$$

$$\frac{\mathrm{d}}{\mathrm{d}t}A_{\mathrm{b}} = k_{\mathrm{b}}\left(\frac{\widehat{B}_{\max}(A_{\mathrm{int}}/V_{\mathrm{int}})^h}{(A_{\mathrm{int}}/V_{\mathrm{int}})^h + K_{\mathrm{M}}^h} - A_b\right) - \widehat{k}_{\mathrm{deg}}A_{\mathrm{b}}, \tag{32}$$

where A_{pl}, A_{int} and A_{b} represent the amount of therapeutic protein in the plasma, interstitial and binding compartment, respectively; V_{int} the interstitial volume, k_{pi} and k_{ip} the rate constants for transfer between the plasma and interstitial compartment, k_{b} the rate constant for binding to and dissociation from EGFR, and k_{el} the elimination rate constant. Furthermore, $\widehat{k}_{\mathrm{deg}}$ denotes the rate constant for elimination by EGFR internalization and degradation, $\widehat{B}_{\max}$ the maximal binding capacity of the therapeutic protein to EGFR, K_{M} the concentration corresponding to $\widehat{B}_{\max}/2$, and h the Hill factor. The initial amount of drug $A_{\mathrm{pl}}(0)$ and the parameters are listed in Table 3. The reported value of K_{M} = 5 μg/ml did not allow us to reproduce the results in [11, Fig.1A]. Only a value of K_{M} = 0.5 μg/ml exactly reproduced the in silico data, hence we choose the corrected value for subsequent analyses. Amounts are converted to concentrations by dividing by the corresponding volume.

Transforming the system of ODEs (30)–(32) from units [mg/kg] to [mg/ml] by dividing by the corresponding volumes yields equations for $C_{\mathrm{pl}} = A_{\mathrm{pl}}/V_{\mathrm{pl}}$, $C_{\mathrm{int}} = A_{int}/V_{\mathrm{int}}$, $C_{\mathrm{b}} = A_{\mathrm{b}}/V_{\mathrm{int}}$, in terms of the following scaled parameters $q_{12} = V_{\mathrm{pl}} \cdot k_{\mathrm{pi}}$, $q_{21} = V_{\mathrm{int}} \cdot k_{\mathrm{ip}}$, $\mathrm{CL}_{\mathrm{lin}} = k_{\mathrm{el}} \cdot V_{\mathrm{pl}}, B_{\max} = \widehat{B}_{\max}/V_{\mathrm{int}}$, $\mathrm{CL}_{\mathrm{RS}} = \widehat{k}_{\mathrm{deg}} \cdot V_{\mathrm{int}}$. The model (30)–(32) scaled to units [mg/ml] can be directly compared to our PK model (20)–(23) with $C_1 = C_{\mathrm{pl}}$, $C_{\mathrm{ex}} = C_{\mathrm{int}}$ and $C_{\mathrm{RS}} = C_{\mathrm{b}}$, parameterized with the scaled parameters above. We remark that alternatively, our compartmental PK models could have been stated in units [mg/kg].

[1] The originally published equations in [11, Supplement] are identical to a certain discretization of the system of ODEs (30)–(32). The advantage of stating the system as continuous ODEs is that subsequently any numerical scheme can be used to solve them, in particular high accuracy ODE solver with adaptive step size control.

Table 3 Parameter values used by Lammerts van Bueren et al. [11]

Parameter	Numerical value
V_{pl}	35 ml/kg
V_{int}	70 ml/kg
$\widehat{B}_{\mathrm{max}}$	2 mg/kg
k_{ip}	0.043 1/h
k_{pi}	0.043 1/h
k_{b}	0.069 1/h
k_{el}	0.0055 1/h
$\widehat{k}_{\mathrm{deg}}$	0.005 1/h
K_{M}	0.5 μg/ml
$A_{\mathrm{pl}}(0)$	2 and 20 mg/kg
h	1.0

K_{M} has been corrected, see text for details. V_{pl} represents the plasma volume

Results

RME for the EGF/EGFR system: an example for ligand–receptor interaction

For all subsequent in silico studies, the parameter values are stated as given in section "EGFR system with endogenous/physiological ligand", unless stated otherwise.

Influence of receptor system properties on RME

We illustrate the approximation features of the two reduced models for predicting concentration-time profiles of the ligand in comparison to the detailed model based on the EGF/EGFR system. The initial concentration is $C_{\mathrm{ex}}(0) = 40$ nM. In Fig. 4(left), the predictions of the extracellular EGF concentration C_{ex} is shown for the three Models A, B and C. All models result in very similar concentration-time

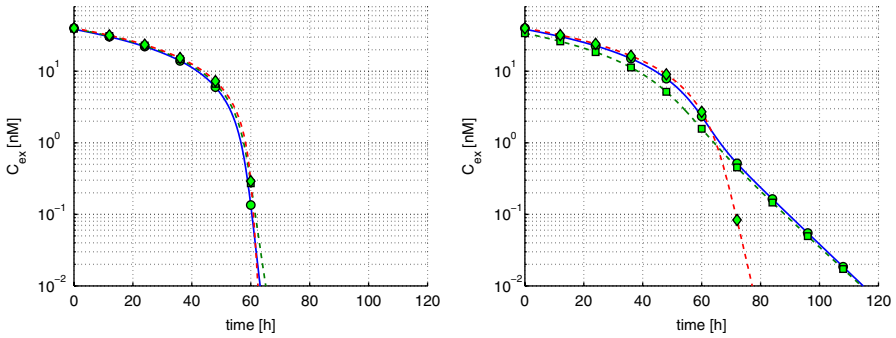

Fig. 4 Concentration-time profile of the extracellular ligand concentration for the Model A (*circles* on blue solid line), Model B (*squares* on blue dashed line) and Model C (*diamonds* on red dashed line). *Left*: Parameter values used according to Table 2. *Right*: As in left figure, but decreasing k_{degRL} 10-fold

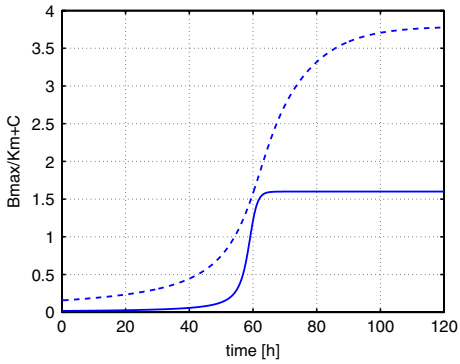

Fig. 5 Evolution of the ratio $B_{\max}/(K_M + C_{\text{ex}})$ for the two scenarios shown in Fig. 4 left (solid line) and right (dashed line)

profiles: Almost instantaneously, the amount of ligand in the RS is in equilibrium. Due to the high concentration of ligand in comparison to the concentration of receptor, the RS is saturated and the ligand is eliminated at a constant rate. Between approximately 40-60 h, the system undergoes a transition from saturated to non-saturated elimination, which is manifested in the linear decline in the final phase (in the semi-logarithmic representation). For the EGF/EGFR system, the detailed model of RME is well approximated by Model B and also by Model C, the latter taking into account only the apparent saturable elimination. Based on the predictions of Model B, we computed the amount of ligand L_{RS} in the receptor system. In accordance with Eq. 15, L_{RS} is negligible in comparison to extracellular EGF concentration (cf. Fig. 5, solid line) while $C_{\text{ex}} > 0.01$ nM.

In order to study the impact of L_{RS} on the approximation quality of Model C, we artificially decrease k_{degRL} by a factor of 10. All other parameters of the detailed Model A, including the initial EGF concentration, are identical. Parameters of Model B and C have been recalculated according to Eqs. 12–14 and Eqs. 19 and 13, respectively, resulting in particular in an increased maximal binding capacity $B_{\max}$. The predictions of the concentration-time profile of the extracellular EGF concentration C_{ex} based on the three Models A, B and C are shown in Fig. 4(right). While Models A and B give almost identical results, the prediction based on Model C differs significantly. Model C over-predicts the extent of elimination by RME. As shown in Fig. 5 the over-prediction corresponds to periods in time where the assumption (15) is violated: While $B_{\max}/(K_M + C_{\text{ex}})$ is small for both settings up to time 60 h, it starts to increase thereafter, in particular for the setting corresponding to Fig. 4(right).

Influence of different cell types on RME

The detailed model A allows us to analyze the influence of processes on the overall disposition of ligand in the extracellular space such as, e.g., the ligand receptor internalization rate constant k_{interRL}. Alterations in k_{interRL} have been observed experimentally [37, 38] and could be the result of a mutation of the EGF receptor. In view of Eq. 28 we would expect a decrease in the overall elimination capacity with decreasing internalization rate constant k_{interRL}. Figure 6(left) shows the impact of

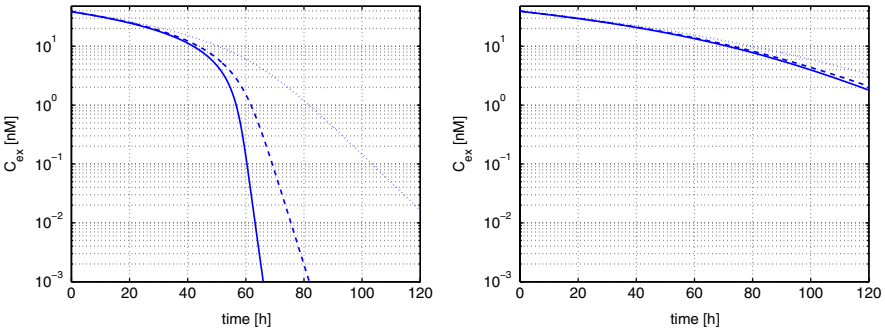

Fig. 6 Illustration of the dependence of RME on the rate of internalization using the detailed model of RME (Model A). Parameter values according to Table 2. *Left*: concentration-time profiles of the extracellular ligand EGF (L_{ex}) for three different internalization rate constants of the ligand–receptor complex: $k_{interRL}$ (*solid line*), $k_{interRL}/4$ (*dashed line*), $k_{interRL}/16$ (*dotted line*). *Right*: same as before, but with decreased association and dissociation rate constants: $k_{on}/100$ and $k_{off}/100$, respectively. Note that K_D is identical in the left and right graphics

an altered $k_{interRL}$ on the concentration-time course of EGF with $C_{ex}(0) = 40$ nM. As can be seen, cells with a reduced internalization rate constant $k_{interRL}/4$ and $k_{interRL}/16$ show a much lower apparent elimination than the reference cells with the rate constant $k_{interRL}$. The difference in the apparent elimination does not only depend on the absolute magnitude of change of $k_{interRL}$, but more precisely on the magnitude of change of $1/k_{interRL} \cdot (1 + k_{recyRL}/k_{lyso})$ in relation to $1/k_{off}$, as can been inferred from Eq. 29. Changes in $k_{interRL}$ will have less impact, if $1/k_{off}$ is large. This can be seen in Fig. 6(right), which shows the same situation as in the left figure, but with k_{off} decreased by a factor of 100 (we also decreased k_{on} by the same factor in order to keep K_D constant).

RME in the monoclonal antibody/EGFR system: an example for therapeutic protein–receptor interaction

In this section we will illustrate how our unified theoretical approach to RME allows for resolving seemingly contradictory statements about the performance of empirical models of RME. In [11], Lammerts van Bueren et al. reported about a preclinical study involving a mAb against EGFR in monkeys and their subsequent data analysis. They developed a two-compartment pharmacokinetic model comprising a first-order elimination of the mAb from plasma, a binding compartment (representing EGFR-expressing cells) that equilibrates with the interstitial compartment, and a saturable internalization and degradation of bound mAb. For a detailed description of the model and the corresponding parameters see section "EGFR system with exogenous/therapeutic protein ligand". Lammerts van Bueren et al. concluded that the observed nonlinear decrease of mAb concentrations in cynomolgus monkeys could not be explained by a saturable elimination in terms of a Michaelis–Menten model and proposed an alternative model, which described the data well. In a different study, the Michaelis–Menten

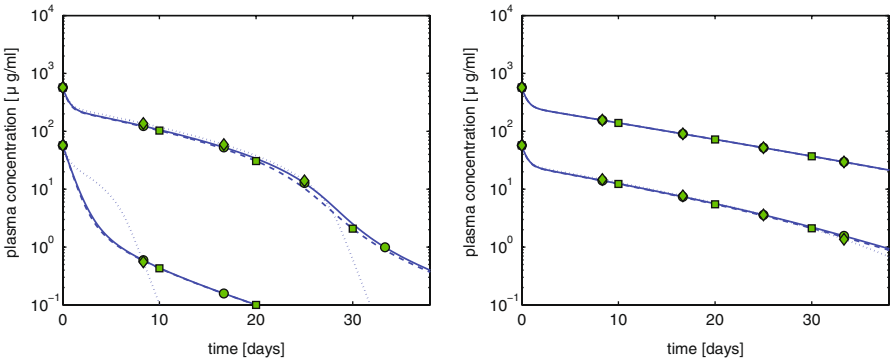

Fig. 7 Comparison of model predictions for zalutumumab (2F8) based on the Lammerts van Bueren et al. model (circles on solid line) and the herein proposed compartment models (20)–(23) (*squares* on solid line) and (24)-(25) (*diamonds* on dotted line). *Left*: parameterization as given in Table 3. *Right*: maximal receptor capacity $B_{\max}$ decreased to one 20th of the original capacity

model was reported to successfully describe in vivo data for a monoclonal antibody [10].

The model proposed in [11] is comparable to the two-compartment model introduced in the section "Integration of RME into compartmental PK models", Eqs. 20–23. In order to understand the inferences made by Lammerts van Bueren et al. [11], we simulated their model defined in Eqs. 30–32 and compared the results to the correspondingly parameterized Models B and C (see Fig. 7, left). Since the experimental data presented in [11] were not available and since model simulations and data were reported to be in good agreement, we used the Lammerts van Bueren model as a surrogate for the experimental data. As in [11], we choose a high and low initial mAb input of 2 and 20 mg/kg. While the predicted mAb plasma concentrations based on Model B are identical to the prediction based on the Lammerts van Bueren et al. model, predictions based on Model C deviate significantly. A closer inspection reveals that the assumption $B_{\max}/(K_M + C_{\mathrm{ex}}(0)) \ll 1$ is violated for the low dose of 2 mg/kg. Consequently, the amount of mAb inside the RS cannot be neglected and we would expect to see deviations between predictions based on Models B and C. Hence, the use of a Michaelis–Menten based nonlinear elimination in the interstitial compartment, which neglects the drug distributed into the receptor system, leads to an over-prediction of drug elimination by RME (see Fig. 7, left).

The difference between the predictions based on Model B and C should disappear, if the maximal binding capacity is sufficiently decreased. This is shown in Fig. 7(right), where the binding capacity $B_{\max}$ has been decreased to one 20th of its original value.

In summary, the inference made in [11] that a Michaelis–Menten term is not adequate for modeling the nonlinearity present in the data is valid for the specific conditions of their experimental design. However, this cannot be generalized to a statement about the validity of the Michael-Menten approximation of RME, as can be seen from Fig. 7(right) and also from the results presented in section "RME for the EGF/EGFR system".

Discussion

Drugs that demonstrate nonlinear pharmacokinetic behavior at therapeutic concentrations often cause difficulties in designing dosage regimens and determining relations between drug concentrations and effects. The theoretical bases and potential causes of nonlinear/dose-dependent pharmacokinetics are many-fold and have been extensively reviewed (see [17] and reference therein). Therapeutic proteins bind with high affinity to specific targets. For many protein drugs elimination by RME plays a major role in their elimination from the body [3]. RME is suspected to be a major source for the nonlinear pharmacokinetic behavior that is observed in pre-/clinical data of numerous protein drugs [6]. In this article we theoretically investigated the process of RME on the pharmacokinetics of therapeutic proteins.

The detailed Model A (see Fig. 1) represents RME for an endogenous compound in terms of a system of biochemical reactions (1)–(5), including the binding of the ligand to the receptor, subsequent internalization of the complex and eventually degradation as well as receptor recycling, degradation and synthesis. Two reduced models have been derived under the assumption that the redistribution processes between the receptor species R_m, RL_m, R_i and RL_i are in quasi-steady-state. For the EGFR system, this assumption has been shown experimentally [27]. For other receptor systems, the steady state assumption seems reasonable since intracellular processes are typically much faster than the time scale of interest in pharmacokinetic studies.

With respect to the pharmacokinetics of therapeutic proteins, two aspects of RME are of particular importance:

1. Distribution as a consequence of the drug binding to the receptor and subsequent internalization of the complex; and
2. Elimination as a consequence of endocytosis.

Unfortunately both processes typically cannot be differentiated experimentally in pharmacokinetics. Model B explicitly takes into account the amount of drug L_{RS} distributed in the receptor system and the elimination by intracellular degradation, e.g., lysosomes. While the elimination is a linear process in terms of L_{RS}, the distribution into the receptor system itself is a saturable process, specified in terms of B_{max} and K_M. Model C is derived from model B by assuming in addition that L_{RS} is negligible in comparison to the extracellular amount L_{ex}. In view of the above two sub-processes, this is equivalent to the assumption that the distributional aspect of RME can be neglected. Notably, even if the distributional aspect is negligible, the receptor system could still very efficiently transport ligand molecules into the cell, where they are subsequently degraded. This can be explained from Eq. 17. It states that the maximal elimination rate V_{max} is the product of the maximal ligand binding capacity B_{max} and the degradation rate constant k_{deg}. The maximal elimination rate V_{max} may still be large due to a large k_{deg}, even if B_{max} is small. The latter implies a negligible amount of ligand L_{RS} within the receptor system. The receptor system acts as a mechanism that transports ligand molecules into the cell to eventually degrade them. Whether or not the receptor system also serves as a distribution phase

is independent from the elimination aspect. This yields the following guidance for the usage of the two reduced models:

Model B: Elimination *and* distribution of ligand into the receptor system are important processes to be considered.
Model C: The distribution of ligand into the receptor system can be neglected, only the elimination process is important, which in this case is non-linear.

Based on Model B and the computable criterion (15) it can easily be checked whether the condition for the applicability of Model C are fulfilled. This has been demonstrated for the EGF/EGFR system in section "RME for the EGF/EGFR system", see Figs. 4 and 5.

The reduced models are derived under the quasi-steady state assumption that the receptor redistribution processes are much faster than the ligand pharmacokinetics. This assumption is of the same type as the assumption underlying the Michaelis–Menten model of enzyme reactions, where it is assumed that the complex formation, dissociation and catalytic transformation are much faster than the transformation of substrate into product. In order to finally derive reduced models, we have to make an additional assumption on the time-scale of receptor synthesis and degradation. There are three different scenarios: receptor synthesis and degradation is (i) as fast as receptor redistribution (or faster); (ii) slower than the time scale of ligand pharmacokinetics; or (iii) at an intermediate time scale, i.e., comparable or faster than ligand PK but slower than receptor redistribution. The first two scenarios correspond to our *fast* and *slow* scenario. Under these assumptions it is possible to either treat receptor synthesis and degradation the same way as the redistribution processes (in the *fast* scenario) or neglect it and treat the total amount of receptor as a constant (in the *slow* scenario), since in the latter it would not impact the total number of receptors on the time scale of interest. In the third scenario, however, receptor synthesis and degradation would need to be taken into account in terms of an additional ODE. Unless further assumptions are made, this would require to consider the full system of Eqs. 1–5—which is not suitable for PK parameter estimation in clinical trials.

The elimination process of RME is specified in terms of the parameters $V_{\max}$ and K_M. Noteworthy, the maximal elimination rate $V_{\max}$ is *independent* of the processes of complex formation (k_{on}) and dissociation (k_{off}) of the receptor-ligand complex. However, the parameters k_{on} and k_{off} influence the amount of extracellular ligand molecules K_M, at which the elimination rate is half-maximal.

In Fig. 6, we studied the impact of different internalization rate constants k_{interRL} on RME. An altered k_{interRL} could, e.g., result from a mutation in the EGF receptor, as it has been observed experimentally [37]. Our analysis in section "Nonlinear PK caused by RME" shows that the ligand elimination rate is affected by various processes inside the cell. For example, the elimination rate decreases with decreasing complex internalization rate constant, but the difference is much less pronounced for a ligand with decreased association and dissociation rate constants k_{on} and k_{off}—even though the dissociation constant K_D is the same in both scenarios (see Fig. 6, left vs. right). From the detailed Model A, this phenomenon is understandable: given a ligand that forms a complex with rate constant k_{on}, once the

ligand–receptor complex is formed at the membrane, its fate is a balance between dissociation (specified in terms of k_{off}) and internalization (specified in terms of $k_{interRL}$). If, e.g., $k_{off}/k_{interRL} \ll 1$ then the complex will predominantly be internalized. Based on K_D alone, this property of receptor systems can not be observed. The ratio $k_{off}/k_{interRL}$ has recently been introduced as one of two key parameters to characterize different cell surface receptor systems (termed the consumption parameter) [28]. In general, our analysis shows that reduced ligand elimination from the extracellular space can be due to altered processes inside the cell other than the velocity of internalization of the complex. The influences of the processes can be deduced from Eq. 28 and is summarized in Table 1. The nonlinearity increases with parameters that accelerate' the processes of receptor availability at the surface (R_0, k_{recyR}) or that accelerate' the transport and intracellular degradation of extracellular ligand (k_{on}, $k_{interRL}$, k_{lyso}). Counteracting processes (related to the parameters k_{off}, k_{interR}, k_{recyRL}) decrease the extent of nonlinearity.

Target-mediated drug disposition (TMDD) models explicitly account for binding to a target and potential degradation of the resulting complex [16–18]. Although originally developed to describe effects of extensive drug target binding in tissues, TMDD has more recently also gained interest as a model of saturable elimination mechanisms for specific peptide and protein drugs, including RME [6, 18, 19]. Between TMDD and the herein presented approach, there are a number of distinct differences. First, the TMDD approach considers pharmacological target binding as the key process controlling the complex nonlinear processes. Particular features of receptor *trafficking* inside the cell are not taken into account. Second, whenever a drug molecule is degraded in the TMDD setting, both, a drug and a receptor molecule are degraded. In the herein presented approach, degradation of the drug does not necessarily imply degradation of the receptor, since the receptor can be recycled. This is, e.g., an important characteristics for the ligand TNF-α. Third, in [16], a reduced model of TMDD is presented based on a equilibrium assumption. In this reduced TMDD model, the unbound extracellular drug concentration is a function of the total concentration, the total receptor concentration R_{tot} and the *equilibrium* dissociation constant K_D [16, Eq. 11]. In our reduced model B, in contrast, the extracellular drug concentration is a function of the total concentration, the maximal receptor binding capacity B_{max} and the *quasi-steady state* parameter K_M (cf. Eq. 8). As a consequence, the models make qualitatively different predictions. For instance, K_M does not only depend on the ratio of k_{off} and k_{on} (i.e., K_D), but also on the actual magnitude of the two parameters, in addition to the dependence on receptor systems parameters. This implies that two drugs with the same K_D but different k_{off} values might be impacted by RME very differently. This has been illustrated in Fig. 6 (compare left and right graphics) and discussed above.

If the reduced models of RME are used as part of structural PK models to estimate parameters in the course of clinical data analysis, the question arises whether or not the identified RME parameters B_{max}, K_M, k_{deg} and V_{max} allow for a mechanistic interpretation, e.g., whether B_{max} can be interpreted as the maximal RME ligand binding capacity. This question is tightly linked to the question of identifiability of model parameters, sometimes referred to as the inverse problem.

Identifiability has been studied in detail in the context of compartmental models (see, e.g., [39, Chap. 5–9]). In general, the identifiability of model parameters depends on the structural model (number of compartments, compartment to which the RME process is linked, existence of additional routes of elimination, etc.), prior knowledge of model parameters and the quality of the experimental design [39, Chap. 5]. To illustrate this, we used the detailed model to generate a set of simulated data, to which we fitted the reduced Models B and C (data not shown). We found that for a well-designed experiment (i) the estimated parameters of the reduced RME models obey the expected relations (12)–(14) and (19); (ii) that Model C will not result in a good fit, if the condition $B_{\max}/(K_M + L_{\text{ex}}) \ll 1$ is violated. This was the case for the in vitro data shown in Fig. 4(left), as well as for the in vivo data shown in Fig. 7(left), where already the authors in [11] reported that they were not able to fit a Michaelis–Menten based PK model to the experimental data. However, if the experimental design is not adequate, then we would expect—in accordance with the parameter identifiability problem [39, Chap. 5–9]—that the above conditions (i) and/or (ii) are violated. This was the case for the in vitro data shown in Fig. 4(right), where both Model B and Model C could be fitted to the generated data based on Model A, although the condition $B_{\max}/(K_M + L_{\text{ex}}) \ll 1$ was violated (resulting in deviation of the estimated parameters from the expected parameters of 6−20% for Model B and 500% for Model C). Since the criteria in Eq. 15 has not been met, the violation of relations in Eqs. 19 and 13 for Model C is in accordance with our expectations. Furthermore, for the situation corresponding to Fig. 4(right), the expected relation $V_{\max} = k_{\text{deg}} \cdot B_{\max}$ (see Eq. 17) was violated, while it was satisfied for the situation corresponding to Fig. 7(left). These results eventually motivate the following recommendation:

Consistency check: Use both reduced Models B and C to fit the data and check the two conditions (15) and (17):

$$\frac{B_{\max}}{K_M + L_{\text{ex}}} \ll 1 \quad \text{and} \quad V_{\max} = k_{\text{deg}} \cdot B_{\max}. \tag{33}$$

A violation of the conditions might indicate an insufficient experimental design, and/or insufficient convergence of the fitting algorithm (local minimum).

Different empirical models have been proposed and used to model the nonlinear pharmacokinetics of therapeutic proteins [7–15]. While, e.g., a Michaelis–Menten based RME model as part of a PK model allowed for describing data in one PK data analysis (e.g., [10]), it failed to do so in another (e.g., [11]). Due to lack of a sound theoretical basis to understand the different performances of empirical models, this certainly was an unsatisfactory situation. The herein presented analysis gives a thorough background of RME and a clear rationale as to when the proposed reduced models are applicable. In addition, the functional relations between the parameters of the detailed Model A and the reduced Models B and C might also serve as a first step to scale in vitro observations on RME to in vivo predictions of either target mediated disposition or Michaelis–Menten elimination, dependent upon the expression level and turnover of the target.

Acknowledgements The authors are grateful to the reviewers for their valuable comments on the manuscript.

References

1. Meibohm B (2006) Pharmacokinetics and pharmacodynamics of biotech drugs. Wiley-VCH Verlag, Weinheim
2. Kuester K, Kloft C (2006) Pharmacokinetics of monoclonal antibodies. In Meibohm B (ed) Pharmacokinetics and pharmacodynamics of biotech drugs, chapter 3. Wiley-VCH Verlag, Weinheim, pp 45–91
3. Mahmood I, Green MD (2005) Pharmacokinetic and pharmacodynamic considerations in the development of therapeutic proteins. Clin Pharmacokinet 44:331–347
4. Russell-Jones GJ (2001) The potential use of receptor-mediated endocytosis for oral drug delivery. Adv Drug Deliver Rev 46:59–73
5. Sorkin A, Von Zastrow M (2002) Signal transduction and endocytosis: close encounters of many kinds. Nat Rev Mol Cell Biol 3:600–614
6. Tang L, Persky A, Hochhaus G, Meibohm B (2004) Pharmacokinetic aspects of biotechnology products. J Pharm Sci 93:2184-2204
7. Dirks NL, Nolting A, Kovar A, Meibohm B (2008) Population pharmacokinetics of cetuximab in patients with squamous cell carcinoma of the head and neck. J Clin Pharmacol 48:267–278
8. Kuester K, Kovar A, Lüpfert C, Brockhaus B, Kloft C (2008) Population pharmacokinetic data analysis of three phase I studies of matuzumab, a humanised anti-EGFR monoclonal antibody in clinical cancer development. Br J Cancer 98:900–906
9. Mould DR, Sweeney KRD (2007) The pharmacokinetics and pharmacodynamics of monoclonal antibodies—mechanistic modeling applied to drug development. Curr Opin Drug Discov Dev 10: 84–96
10. Kloft C, Graefe E-U, Tanswell P, Scott AM, Hofheinz R, Amelsberg A, Karlsson MO (2004) Population pharmacokinetics of sibrotuzumab, a novel therapeutic monoclonal antibody, in cancer patients. Invest New Drugs 22:39–52
11. Lammerts van Bueren JJ, Bleeker WK, Bøgh HO, Houtkamp M, Schuurman J, van de Winkel JGJ, Parren PWHI (2006) Effect of target dynamics on pharmacokinetics of a novel therapeutic antibody against the epidermal growth factor receptor: implications for the mechanisms of action. Cancer Res 66:7630–7638
12. Ette EI, Williams PJ, Ho Kim Y, Lane JR, Liu M-J, Capparelli EV (2003) Model appropriateness and population pharmacokinetic modeling. J Clin Pharmacol 43:610–623
13. Sheiner LB, Beal SL (1983) Evaluation of methods for estimating population pharmacokinetic parameters. III. Monoexponential model: routine clinical pharmacokinetic data. J Pharmacokinet Biopharm 11:303–319
14. Sheiner BL, Beal SL (1981) Evaluation of methods for estimating population pharmacokinetic parameters. II. Biexponential model and experimental pharmacokinetic data. J Pharmacokinet Biopharm 9:635–651
15. Sheiner LB, Beal SL (1980) Evaluation of methods for estimating population pharmacokinetics parameters. I. Michaelis–Menten model: routine clinical pharmacokinetic data. J Pharmacokinet Biopharm 8:553–571
16. Mager DE, Krzyzanski W (2005) Quasi-equilibrium pharmacokinetic model for drugs exhibiting target-mediated drug disposition. Pharm Res 22:1589–1596
17. Mager DE, Jusko WJ (2001) General pharmacokinetic model for drugs exhibiting target-mediated drug disposition. J Pharmacokinet Pharmacodyn 28:507–532
18. Mager DE (2006) Target-mediated drug disposition and dynamics. Biochem Pharmacol 72:1–10
19. Lobo ED, Hansen RJ, Balthasar JP (2004) Antibody pharmacokinetics and pharmacodynamics. J Pharm Sci 93:2645–2668

20. Hendriks BS, Orr G, Wells A, Wiley HS, Lauffenburger DA (2005) Parsing ERK activation reveals quantitatively equivalent contributions from epidermal growth factor receptor and HER2 in human mammary epithelial cells. J Biol Chem 280:6157–6169
21. Wiley HS, Shvartsman SY, Lauffenburger DA (2003) Computational modeling of the EGF-receptor system: a paradigm for systems biology. Trends Cell Biol 13:43–50
22. Sarkar CA and Lauffenburger DA (2003) Cell-level pharmacokinetic models of granulocyte colony-stimulating factor: implications for ligand lifetime and potency in vivo. Mol Pharmacol 63:147–158
23. De Luca A, Carotenuto A, Rachiglio A, Gallo M, Maiello MR, Aldinucci D, Pinto A, Normanno N (2008) The role of the EGFR signaling in tumor microenvironment. J Cell Physiol 214:559–567
24. Watanabe T, Shintani A, Nakata M, Shing Y, Folkman J, Igarashi K, Sasada R (1994) Recombinant human betacellulin. Molecular structure, biological activities, and receptor interaction. J Biol Chem 269:9966–9973
25. Wells A (1999) EGF receptor. Int J Biochem Cell Biol 31:637–643
26. Harari PM (2004) Epidermal growth factor receptor inhibition strategies in oncology. Endocr Relat Cancer 11:689–708
27. Wiley HS, Cunningham DD (1981) A steady state model for analyzing the cellular binding, internalization and degradation of polypeptide ligands. Cell 25:433–440
28. Shankaran H, Resat H, Wiley HS (2007) Cell surface receptors for signal transduction and ligand transport: a design principles study. PLoS Comput Biol 3:e101
29. Baselga J (2001) The EGFR as a target for anticancer therapy—focus on cetuximab. Eur J Cancer 37(Suppl 4):S16–S22
30. Baselga J (2002) Why the epidermal growth factor receptor? The rationale for cancer therapy. Oncologist 7(Suppl 4):2–8
31. Baselga J (2000) New therapeutic agents targeting the epidermal growth factor receptor. J Clin Oncol 18:54S–59S
32. Goel S, Mani S, Perez-Soler R (2002) Tyrosine kinase inhibitors: a clinical perspective. Curr Oncol Report 4:9–19
33. Raymond E, Faivre S, Armand JP (2000) Epidermal growth factor receptor tyrosine kinase as a target for anticancer therapy. Drugs 60(1):15–23; discussion 41–2
34. Hendriks BS, Opresko LK, Wiley HS, Lauffenburger DA (2003) Coregulation of epidermal growth factor receptor/human epidermal growth factor receptor 2 (HER2) levels and locations: quantitative analysis of HER2 overexpression effects. Cancer Res 63:1130–1137
35. Bleeker WK, Lammerts van Bueren JJ, van Ojik HH, Gerritsen AF, Pluyter M, Houtkamp M, Halk E, Goldstein J, Schuurman J, van Dijk MA, van de Winkel JGJ, Parren PWHI (2004) Dual mode of action of a human anti-epidermal growth factor receptor monoclonal antibody for cancer therapy. J Immunol 173:4699–4707
36. Bastholt L, Specht L, Jensen K, Brun E, Loft A, Petersen J, Kastberg H, Eriksen JG (2007) Phase I/II clinical and pharmacokinetic study evaluating a fully human monoclonal antibody against EGFr (HuMax-EGFr) in patients with advanced squamous cell carcinoma of the head and neck. Radiother Oncol 85:24–28
37. Wells A, Welsh JB, Lazar CS, Steven Wiley H, Gill GN, Rosenfeld MG (1990) Ligand-induced transformation by a noninternalizing epidermal growth factor receptor. Science 247:962–964
38. Reddy CC, Wells A, Lauffenburger DA (1994) Proliferative response of fibroblasts expressing internalization-deficient epidermal growth factor (EGF) receptors is altered via differential EGF depletion effect. Biotechnol Prog 10:377–384
39. Godfrey K (1983) Compartmental models and their application. Academic Press, London